Design, Construction and Test of a Double Bitter Magnet

Design, Construction and Test of a Double Bitter Magnet*

Akira Hoshi, Minoru Kudo, Kuniaki Sai, Yoshimi Ishikawa,
Shigeto Miura and Yasuaki Nakagawa
The Research Institute for Iron, Steel and Other Metals

(Received July 19, 1982)

Synopsis

A Bitter magnet with concentric double coils is more efficient than a single-coil magnet especially at a high level of power consumption. The newly constructed double Bitter magnet has been tested up to the power of 3 MW. Some results of mechanical tests for conductor and insulator materials are also described.

I. Introduction

In an earlier paper[1] (hereafter referred to as A), the design, construction and test of a small Bitter magnet usable for a hybrid magnet were reported. A coil of this magnet has an outer diameter of 182 mm and an inner diameter of 37 mm, giving a field of 12.4 T with electric power of 2.99 MW and cooling water of 130 m^3/h. If this will be inserted into a large-bore superconducting coil, the field at the center will exceed 20 T. If more electric power and more cooling water are available, on the other hand, another Bitter coil can be placed instead of the superconducting coil, forming a double Bitter magnet, as has been designed at MIT[2] and Grenoble[3].

The present paper describes the double Bitter magnet firstly constructed at our institute, where the DC electric source and the deionized water cooling system will be enlarged to 8 MW and 350 m^3/h, respectively, in the near future.

The higher the magnetic field generated, the severer becomes the problem of electromagnetic force exerted on the coil. Conductors and insulators must endure strong tension and compression. Their mechanical properties have been examined separately. Some results are described in Appendix.

---

* The 1746th report of the Research Institute for Iron, Steel and Other metals.

II. Design

Parameters for two concentric coils of the double Bitter magnet are defined in Fig. 1. A magnetic field (flux density) produced at the center is given by[4)]

$$B = G_1 \sqrt{W_1 \lambda_1 / \rho_1 a_1} + G_2 \sqrt{W_2 \lambda_2 / \rho_2 a_2} \quad , \tag{1}$$

where W_1 and W_2 are electric powers consumed in the inner and outer coils, respectively. The geometrical factor G_i (i = 1 and 2) depends on not only α_i and β_i but also the distribution of cooling holes. Provided that the total power W (= $W_1 + W_2$) is constant, the maximum field is attained under the following condition:

$$W_1/W_2 = G_1^2 \lambda_1 \rho_2 a_2 / G_2^2 \lambda_2 \rho_1 a_1 \quad . \tag{2}$$

If the two coils are similar to each other i.e. $G_1 = G_2$, $\lambda_1 = \lambda_2$ and $\rho_1 = \rho_2$, the power must be inversely proportional to the dimension i.e. $W_1/W_2 = a_2/a_1$. In fact, however, there must be more cooling holes in the inner coil than in the outer coil, i.e. $\lambda_1 < \lambda_2$. It has been chosen in the present design that $W_1/W_2 \approx 1$.

The electrical connection of the two coils has been made parallel, so the current and the voltage of each coil bear the following relations: $I_1 + I_2 = I$, $V_1 = V_2 = V$. Also the flow of cooling water through the two coils may be either parallel or series. The parallel flow has been chosen here. The flow rate and the pressure difference are as follows: $F_1 + F_2 = F$, $\Delta P_1 = \Delta P_2 = \Delta P$.

Dimensions of the present coils are listed in Table I. Inner and outer radii of the inner coil are the same as those of the small Bitter magnet described in A. Also a pattern of cooling holes and tie-rod holes has been chosen to be the same, since the punch and die are available. The outer coil has been designed so as to utilize the punch and die for one of our old magnets[5)]. Its inner radius, however, must be enlarged afterwards. The electric resistance of the coils is adjusted by the thickness of conductor disks.

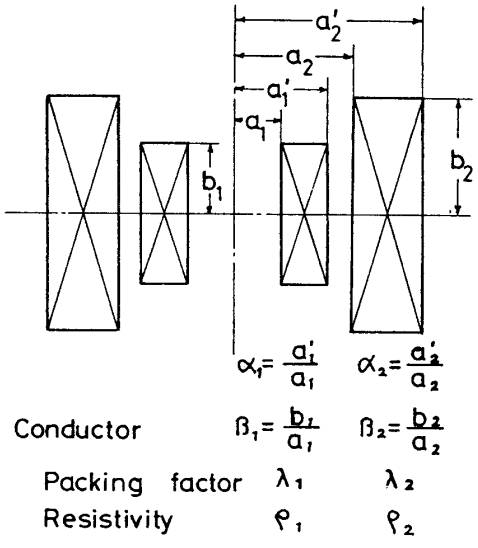

Fig. 1. Parameters for the double Bitter magnet.

Table I. Dimensions (mm) of the double Bitter magnet

	Inner radius	Outer radius	Half height	Disk thickness Conductor	Insulator
Inner coil	18.5	91	46	0.35	0.1
Outer coil	93.5	190	133	0.8	0.1

The electric current and the magnetic field of each coil can be evaluated with eqs. (3) and (4) in A. The number of conductor disks is given by $N = 2b/(t + t')$, where 2b is the height, t and t' are disk thicknesses of conductor and insulator, respectively. Assuming V = 320 (V) and $\rho = 2.2 \times 10^{-8}$ (Ω), we obtain $I_1 = 5.1$ (kA), $W_1 = 1.6$ (MW) and $B_1 = 9.2$ (T) for the inner coil; $I_2 = 4.5$ (kA), $W_2 = 1.4$ (MW) and $B_2 = 4.0$ (T) for the outer coil; hence, W = 3 (MW) and B = 13 (T).

A relation between the flow velocity and the pressure difference of cooling water is given by eq. (5) in A, where the friction factor, f, is assumed to be 0.06. The flow rate, F, is a product of the flow velocity and the total area of cooling holes. Assuming $\Delta P = 1.5$ (kg/cm^2), we obtain $F_1 = 60$ (m^3/h) and $F_2 = 87$ (m^3/h). The temperature rise of water flowing through each coil is calculated as $\Delta T_1 = 23$ (°C) and $\Delta T_2 = 14$ (°C) at the above power, since it is simply derived from the heat capacity of water that

$$\Delta T_i = 860\ W_i/F_i \quad , \quad (i = 1 \text{ and } 2) \tag{3}$$

where ΔT_i is in °C, W_i in MW and F_i in m^3/h. The difference in water temperature between outlet and inlet of the magnet is given as $\Delta T = 860\ (W_1 + W_2)/(F_1 + F_2) = 18$ (°C).

The temperature rise of the conductor depends on the heat-transfer coefficient, H, between the conductor and water. It has been assumed in A that $H = 1.25 \times 10^4\ v$, where v is the flow velocity in m/s and H is in $W/m^2°C$. The temperature difference between the conductor and water may amount to 66 °C and 18 °C for the inner and outer coils, respectively, at the above powers and flow rates. Considerations of the mechanical stress due to the electromagnetic force are given in a later section.

III. Construction

Conductor disks for the inner and outer coils were made of 1 H (full hard) and 1/4 H copper plates, respectively. The yield strength

of the former is higher than that of the latter, as shown in Appendix. Insulator disks were made of glass-fiber-enforced polyimide sheets. These disks were stacked and supported in such a manner as described in A. The inner and outer coils consist of 204 and 295 sheets of conductor disks, having 187.0 and 270.4 turns, respectively. At upper and lower ends of the coils, however, the overlapping angle of the conductor sheets is gradually increased so as to convert spiral current into vertical current smoothly. Thus the effective height of the coil and the number of turns become somewhat smaller.

The double coils were placed inside a heavy brass case, as shown in Fig. 2. Arrows in the figure indicate the flow of cooling water. There are a number of potential leads and thermocouples to measure the temperature rise of conductors and water, although not shown in the figure. Figure 3 shows a photograph of the Bitter disks. The magnet under construction is exhibited in Figs. 4 and 5. An external appearance of the magnet after completion is shown in Fig. 6.

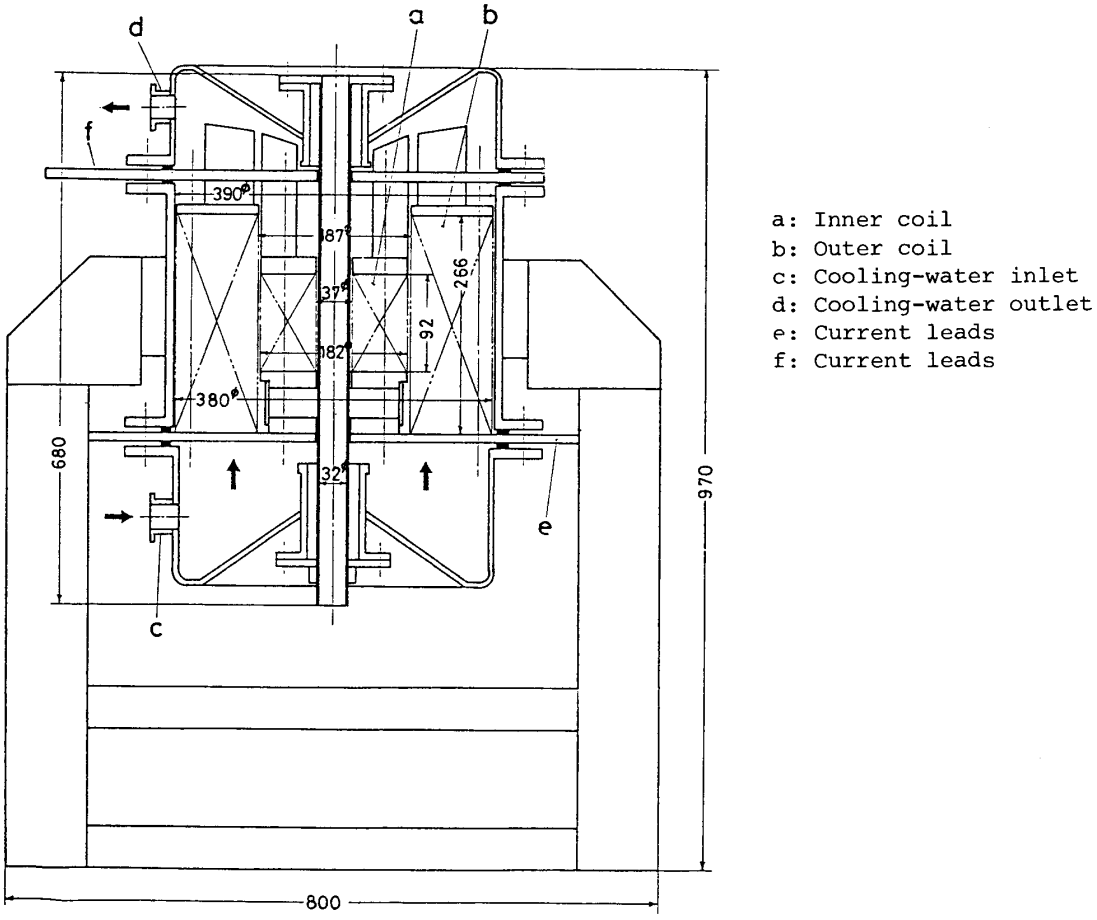

Fig. 2. Cross section of a double Bitter magnet. (Dimensions are in mm.)

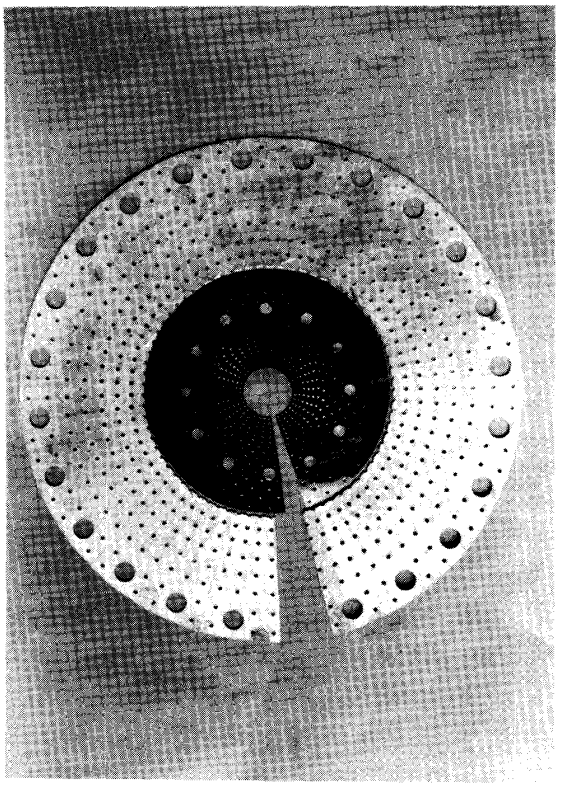

Fig. 3. Disks of a double Bitter magnet.

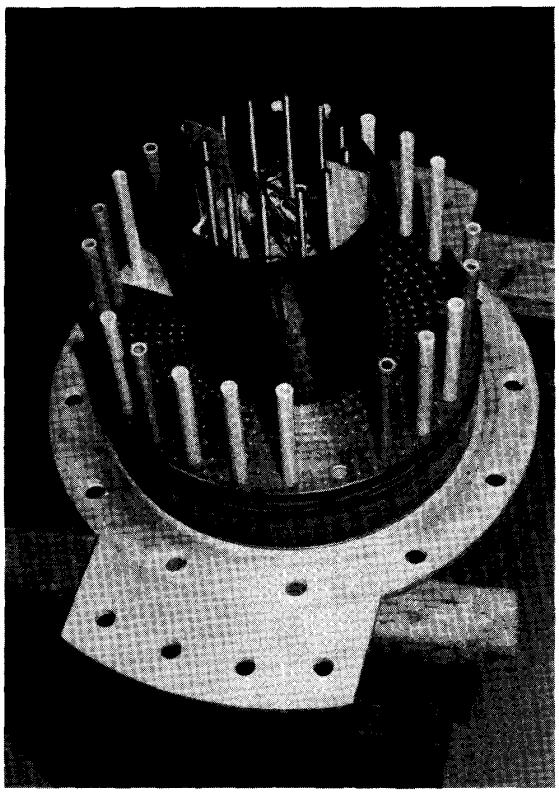

Fig. 4. Magnet under construction (1).

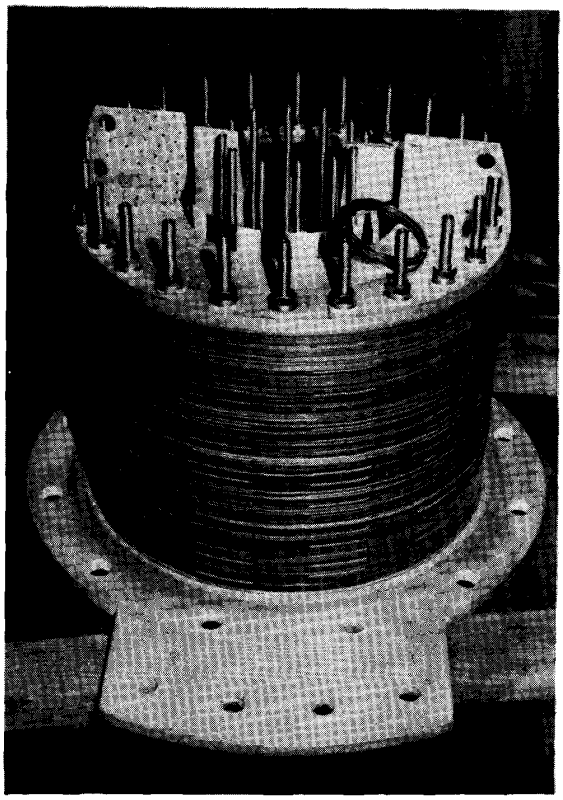

Fig. 5. Magnet under construction (2).

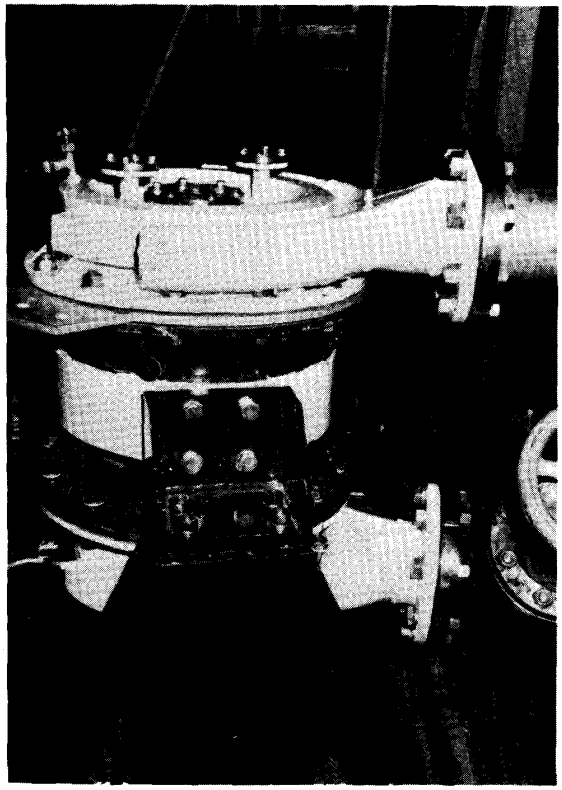

Fig. 6. Magnet after completion.

IV. Test

A flow test of cooling water was made first. Since the flow resistance of this double Bitter magnet was smaller than that of the single Bitter magnet described in A, the total flow rate amounted to 150 m^3/h. Although partial flow rates through the inner and outer coils are difficult to be measured directly, they are estimated from a temperature rise of water flowing through each coil under operation, as shown later.

In order to measure the voltage-current-field relation each coil was energized separately while the cooling water flowed always through the two coils, the flow rate being 150 m^3/h. The initial temperature, T_0, was 24 °C, measured with a thermocouple inside the inlet pipe of water. Figure 7 shows the voltage vs current curves. They are convex upwards, so the resistance increases with the power, as shown in Fig. 8, from which the average temperature rise of the conductor can be estimated. Since the temperature coefficient of resistivity of copper at 24 °C is known as 3.44×10^{-3}/°C, the temperature rise is calculated as 41 °C for the inner coil and 42 °C for the outer coil at the power of 1.7 MW.

The temperature gradient in the conductors could be measured using a number of potential leads of the coils, as fully explained in A. The results are shown in Fig. 9(a) and (b) for the inner and outer coils, respectively. The larger the electric power consumed, the steeper becomes the temperature gradient in the coil. The temperature

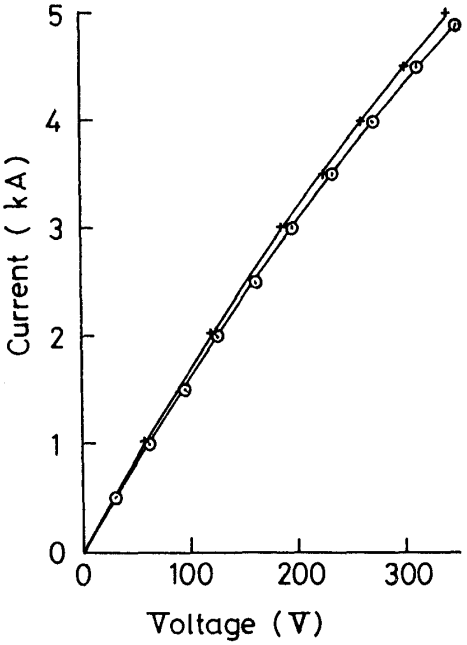

Fig. 7. Current vs voltage.
○ Inner coil. + Outer coil

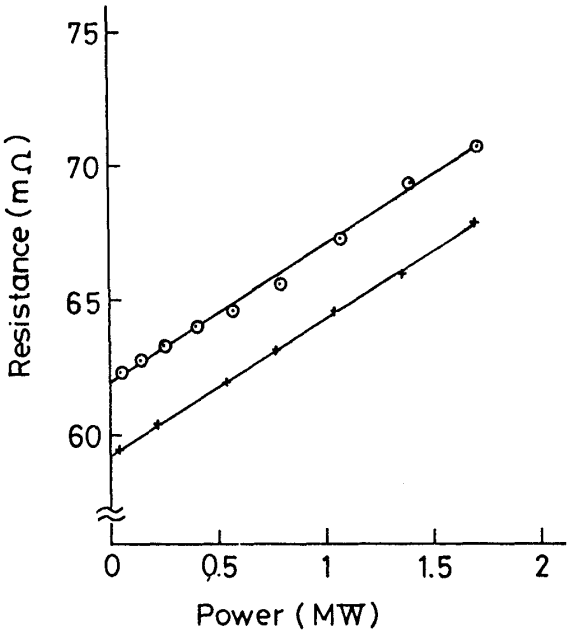

Fig. 8. Resistance vs power.
○ Inner coil. + Outer coil.

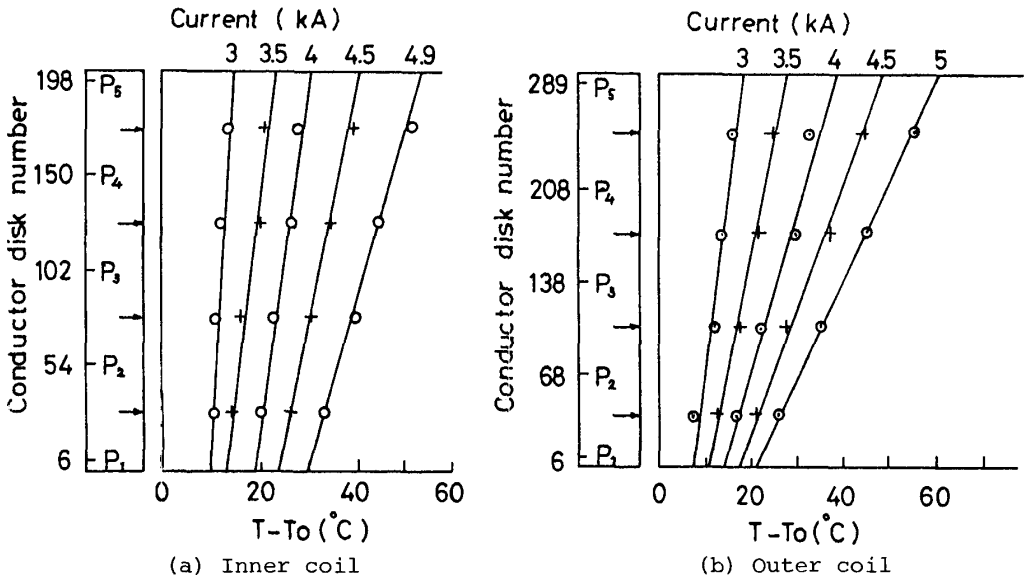

Fig. 9. Temperature distribution in the coil estimated from the resistivity change between potential leads P_i. Arrows indicate mid points of the adjacent leads. T_0 is the initial temperature, 24 °C.

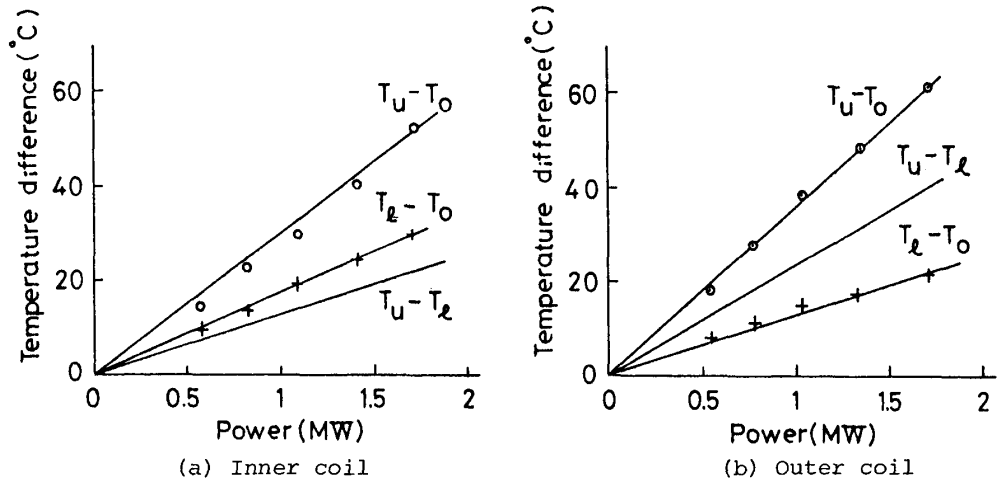

Fig. 10. Temperatures of conductors at upper end (T_u) and lower end (T_ℓ) of the coil. T_0 is the initial temperature, 24 °C.

rise, $T - T_0$, at the center of each coil agrees with the average temperature rise mentioned above. The values at upper and lower ends of the coil, $T_u - T_0$ and $T_\ell - T_0$ respectively, are obtained by extrapolation, and plotted against the power in Fig. 10(a) and (b). The temperature difference between the conductor and water corresponds to $T_\ell - T_0$, being larger in the inner coil than in the outer coil, as has been expected in the design.

Figure 10 also shows $T_u - T_\ell$ which should be equal to the temperature difference of water between the upper and lower ends, i.e. ΔT_i in eq. (3). The value of $T_u - T_\ell$ for the inner coil, 22 °C at 1.7 MW,

is in satisfactory agreement with the expected value of ΔT_1, while $T_u - T_\ell$ for the outer coil, 40 °C at 1.7 MW, is much larger than the expected value of ΔT_2, indicating that the partial flow rate through the outer coil, F_2, is much smaller than that of the inner coil, F_1. This is probably caused by anomalous water flow through an annular gap between the case and the outer coil, i.e. an appreciable amount of water flows into the outer coil, runs out through the slit of the Bitter disks at the lower part, pours into the annular gap, and then arrives at the outlet pipe directly.

Figure 11 shows the distribution of magnetic fields. The voltage applied to each coil was kept at 200 V. The field produced by each coil, B_1 & B_2, was maximum at the geometrical center, and symmetrically decreased along the central axis. This is essential for the double Bitter magnet, since the electromagnetic force between the two coils must be cancelled. The field B produced by the simultaneous operation of the two coils at 200 V is also shown in the figure. It is to be noted that B was about 1.3 % larger than $B_1 + B_2$, since B was measured on another day when the initial temperature of cooling water, T_0, was 20 °C, lower than that mentioned above.

The field is proportional to the current which varies with the voltage as shown in Fig. 7. Figure 12 shows the field at the center plotted vs voltage for the individual and simultaneous operations of the two coils. The data shown in Figs. 7 and 12 are summarized as follows: if V = 330 (V) and T_0 = 24 (°C), then I_1 = 4.73, I_2 = 4.89 and I = 9.62 (kA); W_1 = 1.56, W_2 = 1.61 and W = 3.17 (MW); B_1 = 8.2,

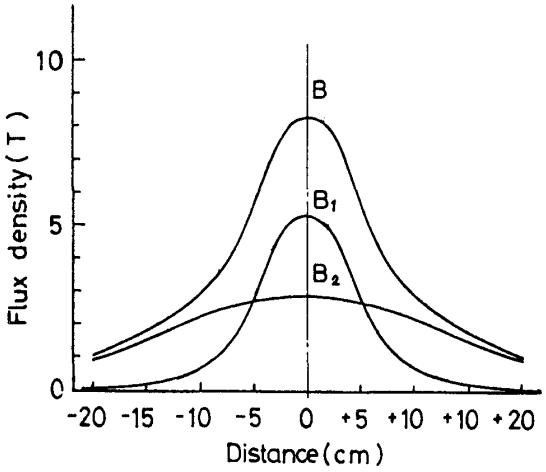

Fig. 11. Field distribution along the central axis at the voltage of 200 V.
B_1: inner coil.
B_2: outer coil.
B : double coils.

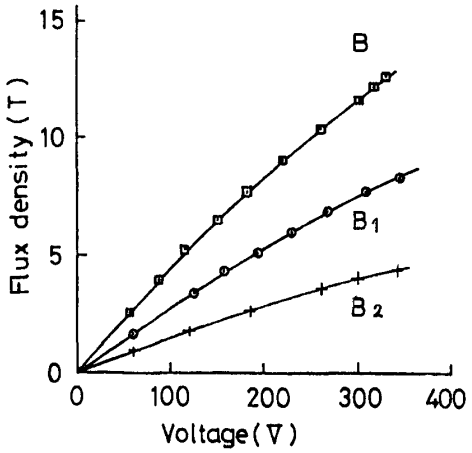

Fig. 12. Magnetic field (flux density) at the center vs voltage.
B_1: inner coil.
B_2: outer coil.
B : double coils

B_2 = 4.3 and B = 12.5 (T). The current and field of the inner coil are fairly smaller than those estimated in section II, probably due to an appreciable effect of contact resistance of the conductor disks.

V. Conclusions

The field produced by the present double Bitter magnet is not so different from that of the single Bitter magnet described in A. It should be emphasized, however, that the temperature rise of the conductors was remarkably reduced, so more electric power can be provided to produce higher fields. In addition, the superiority of the double Bitter magnet is clearly understood if the mechanical stress due to the electromagnetic force is also taken into consideration. As was discussed elsewhere[6], the optimum current distribution and the optimum coil shape are determined by thermal and mechanical limitations. It has also been known[7] that the larger the ratio of the outer and inner radii of a Bitter coil, the larger becomes the stress enhancement factors, so the mechanical limitation is much relaxed if the coil is divided into a number of concentric coils which are supported independently. It has been planned, therefore, that another double Bitter magnet with a smaller outer diameter is used for a hybrid magnet in our institute, which possibly produces a total field of 20 T. The present magnet, on the other hand, will serve as the most powerful magnet without superconductors, when more electric power will become available in the near future.

Acknowledgements

The authors are indebted to Mr. H. Hiroyoshi for his cooperation in the test of the magnet and to Mr. Y. Suenaga for the tensile test of the conductors. Thanks are also due to Mr. H. Moriya for preparation of the manuscript. The work has been suported by Grant-in- Aid for Scientific Research (Grant No. 00584009) of the Ministry of Education, Science and Culture.

Appendix

An electromagnetic force exerted on coil materials is proportional to a square of magnetic field. Much greater stress will possibly be imposed on the present magnet when energized with a larger electric source in the future. Therefore, strength tests of the coil materials were made separately.

1. Conductor

The yield strength of conductors for the Bitter disk, 1 H and 1/4 H copper, was measured using a tensile test machine. Two kinds of test pieces were prepared, as shown in Fig. 13. The test piece (a) has two circular holes in order to simulate the stress concentration around cooling holes in the Bitter disk, and the test piece (b) is of a standard type. Both have the same width of 10 mm at the narrowest part. Figure 14 shows stress vs elongation curves measured at a constant elongation rate of 1 mm/min, where the stress, σ, is defined as the force divided by the narrowest cross-section. The maximum values, σ_m, were well reproducible, as indicated in the figure.

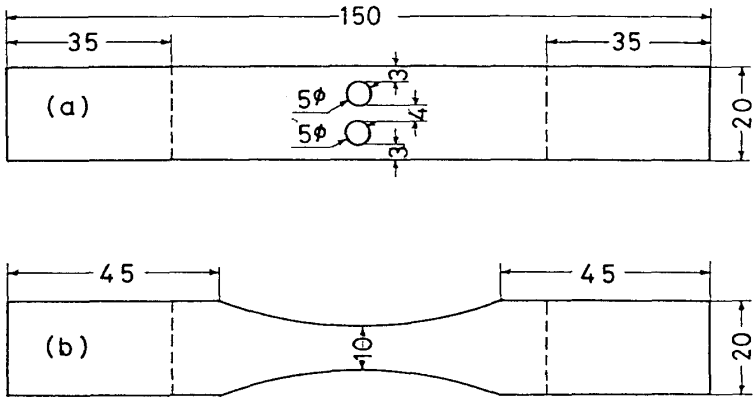

Fig. 13. Test pieces. (Sizes are in mm.)

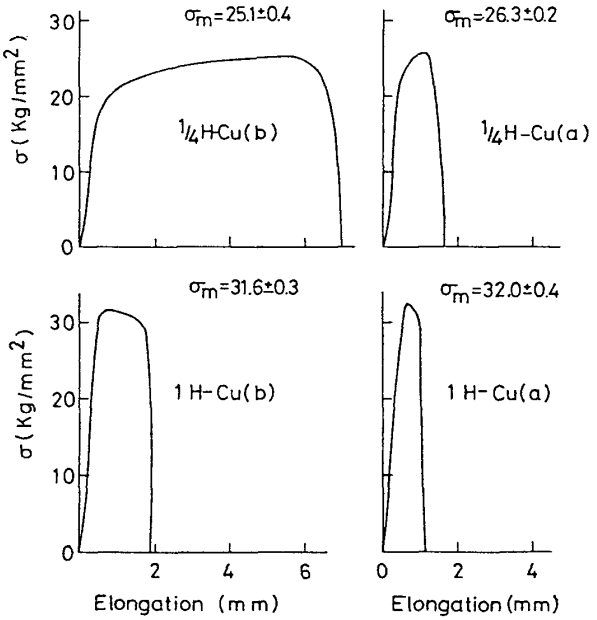

Fig. 14. Stress vs elongation for test pieces (a) and (b).

The test piece (a) was also used for a tensile fatigue test. Figure 15 shows the number of cycles to fracture plotted against the tensile stress. A life time of the Bitter coil can be estimated from this result. For example,

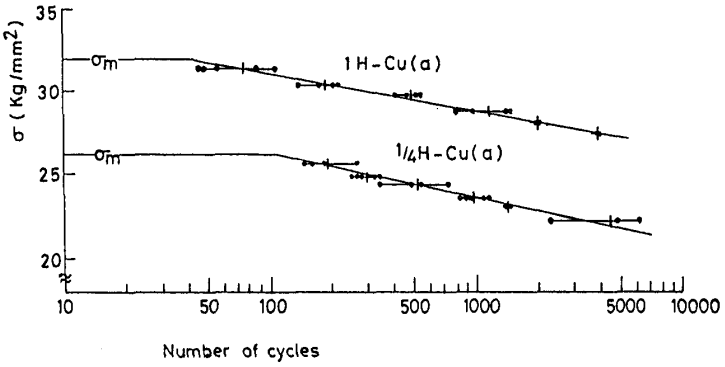

Fig. 15. Fatigue test.

if the maximum stress exerted on the coil made of 1 H copper amounts to 30 kg/mm^2, the coil may be fractured after 200 ∿ 300 cycles of the generation of the maximum field. In fact, the maximum stress of the present magnet has been evaluated as 28 kg/mm^2 for the inner coil and 3 kg/mm^2 for the outer coil when generating a total field of 13 T. Some material stronger than 1 H copper would be indispensable if higher fields should be generated.

2. Insulator

An insulator disk placed between the conductor disks is compressed with the electromagnetic force, so a simulation test on glass-fiber-enforced polyimide sheets was made using a press machine. A test piece was a circular plate of 5.5 mm in diameter with a small circular hole of 2.2 mm in diameter at the center. The pressure was defined as the

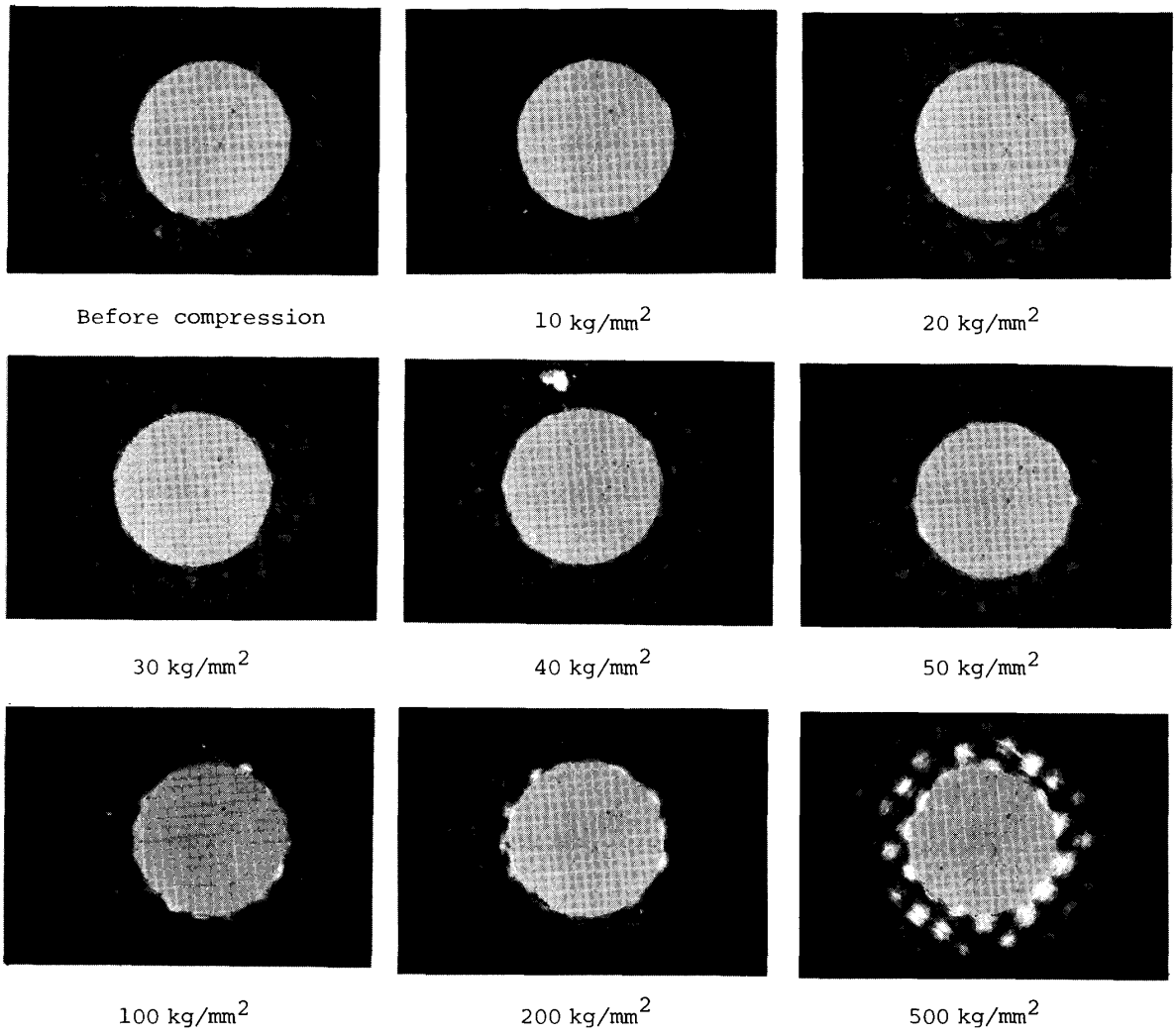

Fig. 16. Compression test for glass-fiber-enforced polyimide sheet. Photographs shows a part of the sheet around a circular hole of 2.2 mm in diameter.

load of the press divided by the area of the piece (20.0 mm^2). After the compression during 30 seconds, the piece was inspected with a microscope. Figure 16 shows photographs of a part around the circular hole. No effect of the compression was observed up to 30 kg/mm^2, a slight change appeared near the hole at 40 kg/mm^2, and a heavy damage was found at 100 kg/mm^2. Since the Maxwell stress, $B^2/2\mu_0$, is 36 kg/mm^2 at the field of 30 T, this sheet is usable even for a hybrid magnet. It is to be noted, however, that the insulator of the Bitter magnet is exposed to hot water and possibly suffers some deterioration.

References

(1) Y. Nakagawa, S. Miura, A. Hoshi, M. Kudo, K. Sai and Y. Ishikawa: Sci. Rep. RITU A30 (1981) 86.
(2) R. J. Weggel: J. Magn. & Magn. Mater. 11 (1979) 321.
(3) J. C. Picoche, P. Rub and H.-J. Schneider-Muntau: ibid. 308.
(4) D. B. Montgomery: Solenoid Magnet Design (Wiley-Interscience, New York, 1969) p. 16.
(5) S. Maeda: High Magnetic Fields, Proc. Int. Conf., MIT, 1961 (Wiley, 1962) p. 406.
(6) Y. Nakagawa: IEEE Trans. Magn. MA-17 (1981) 1786.
(7) Ref. 4), p. 123.